Proceedings of the 2025 Winter Simulation Conference
E. Azar, A. Djanatliev, A. Harper, C. Kogler, V. Ramamohan, A. Anagnostou, and S. J. E. Taylor, eds.

EXTENDING SOCIAL FORCE MODEL FOR THE DESIGN AND DEVELOPMENT OF CROWD CONTROL AND EVACUATION STRATEGIES USING HYBRID SIMULATION

Aaron LeGrand[1] and Seunghan Lee[1]

[1]Dept. of Industrial and Systems Eng., Mississippi State University, Mississippi State, MS, USA

ABSTRACT

Efficient crowd control in public spaces is critical for mitigating threats and ensuring public safety, especially in scenarios where live testing environments are limited. It is important to study crowd behavior following disruptions and strategically allocate law enforcement resources to minimize the impact on civilian populations to improve security systems and public safety. This paper proposes an extended social force model to simulate crowd evacuation behaviors in response to security threats, incorporating the influence and coordination of law enforcement personnel. This research examines evacuation strategies that balance public safety and operational efficiency by extending social force models to account for dynamic law enforcement interventions. The proposed model is validated through physics-based simulations, offering insights into effective and scalable solutions for crowd control at public events. The proposed hybrid simulation model explores the utility of integrating agent-based and physics-based approaches to enhance community resilience through improved planning and resource allocation.

1 INTRODUCTION

Recent increases in threats to the public have drawn the attention of researchers to model such threats. Even though these threats are rare, their consequences can be catastrophic, making the development and validation of control policies a significant challenge. Over the last decade, the number of terrorist attacks and the number of casualties per attack have been increasing, as shown in Figure 1 (De Cauwer et al. 2023). To effectively prepare for future events, we must accurately model previous attacks and future threats to modify procedures and minimize the number of casualties. Therefore, developing robust and relevant models is essential for understanding and mitigating the impact of these threats on public safety.

Simulations can address rare events and can be used to develop control policies. Large crowd models will be key to demonstrating the reality of the elements, which will directly affect the validity of the simulation models. Due to these constraints, simulations must be used to validate control policies to minimize damages from these threats. Correctly modeling crowd evacuation procedures is crucial to understanding the validity of control policy, and there is currently little research about differentiating law enforcement officers from normal pedestrians in evacuation modeling. There are many ways to model crowd evacuations, but the most prevalent one is social force models (SFM) (Helbing and Molnar 1995). SFMs treat each agent as a physics object, producing and receiving forces that dictate their movement and the movements of those around them. SFMs offer distinct advantages and insights, making them invaluable tools in the development of effective evacuation strategies.

This paper addresses the following research question: How can SFM be extended to allow law enforcement personnel to efficiently control crowds, thereby supporting more effective evacuations? This research aims to both incorporate law enforcement crowd control strategies by extending the SFM (E-SFM) and develop a physics-based simulation of crowd evacuation using the E-SFM under evacuation procedures. Our contributions include the addition of a new force and the generation of existing forces within the social force model, applying it to the context of college campus attack evacuations. The proposed approach demonstrates its potential to improve evacuation strategies in such critical scenarios by exploring how law

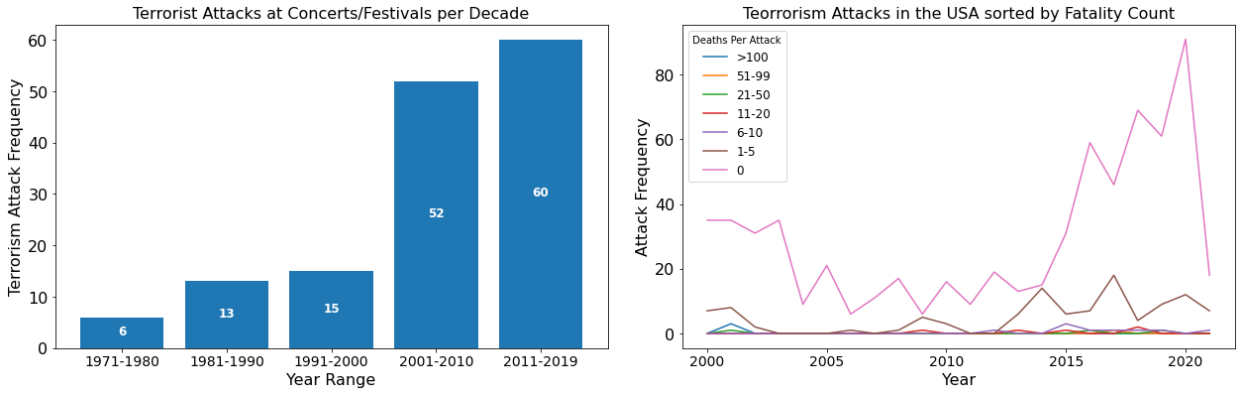

(a) Terrorism Incidents Per Decade till 2019

(b) Casualties per Incident in the US from 2000-2021

Figure 1: Trends in terrorism attacks and casualties.

enforcement can control crowd movement and influence evacuation policies. It will also support developing effective crowd control policies with validation through simulations, providing valuable insights into the efficacy of different control strategies during evacuations.

2 LITERATURE REVIEW

There are three prevalent categories of crowd simulation models (Yang et al. 2020). The first category is microscopic models which focus on the details and smaller parts of the simulation, such as pedestrian-to-pedestrian interaction instead of overall crowd traffic flow. This category includes rule-based (Xiong et al. 2009), force-based, velocity-based (Pettré et al. 2014; Liu et al. 2022), agent-based (Luo et al. 2008), and vision-based models (Ondřej et al. 2010). The next category of models are macroscopic models. These include continuum models (Golas et al. 2014), aggregate dynamics (Narain et al. 2009), and potential field-based models (Xing et al. 2015). Macroscopic models often are not a realistic model due to overlooking pedestrian interaction. The last major category of crowd simulation models are the mesoscopic models, including but not limited to dynamic group behavior models (He et al. 2016), interactive group formation (Zhang et al. 2015), and social psychological crowds (Stokols 1972). While all of these models have their application for different scenarios, we will use a force-based model called the Social Force Model (Helbing and Molnar 1995). Using a SFM allows us to modify individual behavior to incorporate different types of pedestrians in our simulation scene.

Since the initial concept of the SFM was proposed in 1995, many modifications have been made to it to better represent different situations of crowd dynamics. Some of these modifications include grouping (Huang et al. 2018), panicking behavior vs normal behavior (Helbing et al. 2002), evacuation procedures (Wei-Guo et al. 2006; Arteaga et al. 2023), and even considering anxiety levels of the pedestrians during evacuation situations (Cornes et al. 2021). While the initial concept of the SFM was basic, it is easily adaptable to any situation where pedestrian dynamics need to be modeled for a computer simulation. Here, we will cover many different types and functionalities of SFMs to lay the framework for this research. (Wan et al. 2014) used a modified combined SFM to model the emergency evacuation of a subway station after a terrorist attack, in this case, a gas attack. Terrorist attack evacuations are very commonly modeled with SFMs. (Han and Liu 2017) used an SFM to model an attack scenario where the threat is knife-wielding humans located in the attack zone.

SFMs, with consideration of groups of people within the crowd, have been studied by researchers in an attempt to model crowd behavior more accurately. Pedestrians in a group will stay together and return to each other if separated (Kolivand et al. 2021). One article highlights the force that police officers provide during an attack situation (Lu et al. 2023). This effort brings the utilization of virtual reality (VR) to control

the behavior of pedestrians and to gain feedback about a person's affective state across different crowd densities (Dickinson et al. 2019). To implement such evacuation scenarios, the dynamic environmental effects should have been well incorporated. Game engines have often been used to create visually realistic simulation environments (Prasithsangaree et al. 2003; Xin et al. 2024; Zhang et al. 2023). One of the reasons why the game engine is a popular choice for researchers is due to the program's customizability (e.g., from small scale to large scale). For example, small-scale simulations can be built to investigate human performance on small tasks (Xin et al. 2024), such as adjusting scientific equipment inside of a laboratory. On the other hand, simulations on a large scale can be constructed with high levels of detail as well. An example of this is simulating autonomous submarine navigation inside of a 3D ocean environment (Zhang et al. 2023). High levels of detail in a virtual environment allow for new opportunities in research, like extracting synthetic data from simulations.

3 MODELING METHODOLOGY

This section introduces the proposed Extended Social Force Model (E-SFM) and demonstrates the validity of the extension. The extension is the introduction of a *bubble force* $\mathbf{f}_{ik}^{\text{bf}}(t)$ to represent law enforcement personnel's control effects in an evacuation simulation as shown in Figure 2. The bubble force extension is needed because police officers exert a demanding and authoritative presence in a crowd, often causing pedestrians to move out of the officer's way during panicking scenarios. This influence can change the behavior of many pedestrians in a real-life scenario, so it must be modeled correctly. Other extensions we test are modifications to the repulsive force $\mathbf{f}_{ik}^{\text{rf}}(t)$ and the physical force $\mathbf{f}_{ik}^{\text{pf}}(t)$. First, we will outline the basic SFM used to compare against our proposed methodology. The basic SFM used will be a combination of (Helbing and Molnar 1995; Helbing et al. 2002). Firstly, the authors will show the equations used to define the basic SFM. The following subsection will show equations and coefficients to describe the E-SFM.

3.1 Social Force Model

Currently, research in the field of SFMs and modified SFMs builds off of the framework proposed by (Helbing and Molnar 1995). In this section, the authors cover the equations of the SFM before covering any modifications to it. This review is important to outline due to the fact that some of these equations will be modified for the extended methodology. The description of basic SFM is mainly from the two representative work by (Helbing and Molnar 1995; Helbing et al. 2002). This model serves as the baseline against which the E-SFM is compared. This model considers pedestrian dynamics both in a normal and in a panicking state, much like they would be before and after the evacuation begins, respectively. The force equations of the SFM are detailed in Table 1.

3.1.1 Social Force Model Under Normal Conditions

The velocity of pedestrian $i \in I$ at time $t \in T$ is represented by $\mathbf{v}_i(t) \in \mathbb{R}^2$. Velocity is defined by the change in position $\mathbf{x}_i(t) \in \mathbb{R}^2$ (2D plane), given by $\frac{d\mathbf{x}_i(t)}{dt} = \mathbf{v}_i(t)$. After defining the velocity, we can derive the acceleration equation governing pedestrian i with her own mass m_i as follows. Let $\mathbf{f}_i(t) \in \mathbb{R}^2$ be the sum

Table 1: Index and force explanations.

Index	Explanation	Forces	Explanation
$i \in I$	Pedestrian of interest	$\mathbf{f}^{\text{rf}}(t)$	Repulsive Force
$j \in J$	Surrounding Pedestrians	$\mathbf{f}^{\text{bf}}(t)$	Bubble Force
$k \in K$	Law Enforcement Officer	$\mathbf{f}^{\text{pf}}(t)$	Physical Force
$g \in G$	Special Attraction	$\mathbf{f}_i(t)$	Overall Force on Pedestrian i

of all social forces acting on the pedestrian at any time t. Additionally, let $\mathbf{q}_i(t)$ represent fluctuations in the pedestrian's behavior that capture individual movement variability not represented by the model. The individual's acceleration is then represented by:

$$m_i \frac{d\mathbf{v}_i(t)}{dt} = \mathbf{f}_i(t) + \mathbf{q}_i(t) \tag{1}$$

These equations describe how the velocity and acceleration of a pedestrian are influenced by both social forces and individual behavioral fluctuations.

To create a correct simulation of an evacuation scenario, we must differentiate the behavior of the pedestrians before and after the evacuation takes place. (Helbing et al. 2002) created two different force models to define pedestrian dynamics in each situation. The first one we will review is that of the pedestrian behavior in a normal situation (pre-evacuation). Each pedestrian produces a repulsive force as well as an attractive force upon other pedestrians. The repulsive force describes the common behavior of pedestrians maintaining a comfortable distance between others. This force can be represented by $\mathbf{f}_{\mathrm{ij}}^{\mathrm{rf}}(t)$. Equation (2) represents the repulsive force between pedestrians.

$$\mathbf{f}_{ij}^{\mathrm{rf}}(t) = A_i \exp\left(\frac{r_{ij} - d_{ij}}{R_i}\right)\mathbf{n}_{ij}\left(\gamma_i + (1+\gamma_i)(\frac{1+\cos\varphi_{ij}}{2})\right) \tag{2}$$

where $A_i \in \mathbb{R}^+$ is the interaction strength and $R_i \in \mathbb{R}^+$ is the range of the repulsive interactions that depend on each scenario. The variable $r_{ij} = r_i + r_j$ is the sum of the radii of the pedestrian that represents their body size. The distance between two pedestrian's center of mass is given by $d_{ij}(t) = \|\mathbf{x}_i(t) - \mathbf{x}_j(t)\|_2$. Next, we can use the vector n_{ij} to denote the normalized vector that points from pedestrian j to i. The variable γ_i is used to model importance of events happening either in front of or behind them. $0 < \gamma_i < 1$ allows for the events in front of a pedestrian to grasp their attention over things happening behind them. The angle $\varphi_{ij}(t)$, which ranges from 0 to 360°, represents the angle between the direction of motion and the direction of the pedestrian exerting the repulsive force. This angle is defined by the equation $\cos\varphi_{ij}(t) = -\mathbf{n}_{ij}(t)\cdot\mathbf{e}_i(t)$. The vector $\mathbf{n}_{ij}(t)$ can be represented as $\mathbf{n}_{ij}(t) = \left[n_{ij}^1(t), n_{ij}^2(t)\right] = \frac{\mathbf{x}_i(t)-\mathbf{x}_j(t)}{d_{ij}(t)}$, where $\mathbf{n}_{ij}(t)$ is the unit vector pointing from pedestrian j to pedestrian i, $\mathbf{e}_i(t)$ is the unit vector in the direction of motion of pedestrian i, $\mathbf{x}_i(t)$ and $\mathbf{x}_j(t)$ are the positions of objects i and j, respectively, and $d_{ij}(t)$ is the Euclidean distance between pedestrians i and j. This relationship helps in understanding how the direction of motion and repulsive forces are aligned in the context of the social force model.

When pedestrians are not in a panicking situation, i.e. normal behavior, they can be influenced by forces coming from inanimate objects such as windows, lights, stores, etc. The object creating this special attraction can be indexed as $g \in G$. This type of interaction can be represented by the force $\mathbf{f}_{ig}^{\mathrm{att}}(t)$, where i and g illustrate the index of the pedestrian and the special attraction objects, respectively. With this type of interaction, the interaction range R_{ig} is usually larger than with a pedestrian j, but the strength of the interaction A_{ig} is usually smaller, negative, and time-dependent. Equation (2) is used to define $\mathbf{f}_{ig}^{\mathrm{att}}(t)$, but with index ig instead of ij, and significantly different coefficient values of A_{ig} and R_{ig}.

The following force equation for $\mathbf{f}_{ij}^{\mathrm{att}}(t)$ ensures that individuals formed in groups will join again even after being separated. It defines the attraction force between pedestrians i and j: $\mathbf{f}_{ij}^{\mathrm{att}}(t) = -C_{ij}\mathbf{n}_{ij}(t)$ Now, one can present an equation that summarizes all of the social forces that act on pedestrian i. The force $\mathbf{f}_{\mathrm{ib}}(t)$ represents the force between the pedestrian and a boundary b (typically a wall, fence, building, etc., and pushing the pedestrian i away). The vector $\mathbf{e}_i(0)$ represents the initial direction of motion and v_i represents the magnitude of the initial velocity as a scalar: $v_i(0) = \sqrt{v_x^2(0) + v_y^2(0)}$. Lastly, there is a relaxation term τ_i that is used to calculate the acceleration term. The summary of forces on pedestrian i is defined in Equation (3).

$$\mathbf{f}_i(t) = \frac{v_i(0)\mathbf{e}_i(0) - \mathbf{v}_i(t)}{\tau_i} + \sum_{j(\neq i)}\left[\mathbf{f}_{ij}^{\mathrm{rf}}(t) + \mathbf{f}_{ij}^{\mathrm{att}}(t)\right] + \sum_{b\in B}\mathbf{f}_{ib}(t) + \sum_{g\in G}\mathbf{f}_{ig}^{\mathrm{att}}(t) \tag{3}$$

3.1.2 Social Force Model Under Evacuation Conditions

The previous force equations represent pedestrian dynamics in a normal situation. However, we need to model their behavior differently in an evacuation scenario, since the forces they will enact on one another will be different and with a different strength. Researchers have detailed a new set of equations to define pedestrian dynamics when they are in a state of panic, or evacuation (Helbing et al. 2002). This type of representation will work perfectly to represent our simulated pedestrians during an evacuation. The authors dropped attractive effects out of the force equation and set the value for $\gamma_i = 0$.

There is not only a social force here that influences pedestrian behavior, but a physical force as well for when pedestrians come into contact with one another. This happens when $r_{ij} \geq d_{ij}$, or when the sum of the radius of two pedestrian's bodies is larger than the distance between their center of mass, meaning they have come into contact and produce a physical force $\mathbf{f}_{ij}^{\text{ph}}(t)$. The variables r_{ij}, d_{ij},and $\mathbf{n}_{ij}$ remain the same as the normal scenario equations. The first part of the force formula $p(r_{ij} - d_{ij})\mathbf{n}_{ij}$ is the body force counteracting body compression. The second part of the formula $\kappa(r_{ij} - d_{ij})\Delta v_{ji}\mathbf{t}_{ij}$ is a sliding friction force that impedes relative tangential motion. The function $\Theta(z)$ ensures that the value is greater than or equal to 0, where the input is equal to the output unless it is less than 0, then $\Theta(z) = 0$. The vector $\mathbf{t}_{ij} = (-n_{ij}^2, n_{ij}^1)$ is the tangential direction, related to the vector of the object exerting the force $\mathbf{n}_{ij} = (n_{ij}^1, n_{ij}^2)$. The tangential velocity difference is $\Delta v_{ji} = (\mathbf{v}_j - \mathbf{v}_i) \cdot \mathbf{t}_{ij}$. p and κ are large constants corresponding to the body force and the sliding friction force, 1.2×10^5 and 2.4×10^5, respectively (Helbing et al. 2000). Equation (4) represents the physical force produced when two bodies make contact.

$$\mathbf{f}_{ij}^{\text{ph}}(t) = p\Theta(r_{ij} - d_{ij})\mathbf{n}_{ij} + \kappa\Theta(r_{ij} - d_{ij})\Delta v_{ji}\mathbf{t}_{ij} \tag{4}$$

Interactions with boundaries or walls are treated similarly to that of interactions with other pedestrians. The formulation is in the same notation where $\mathbf{f}_{ib}$ represents the force between pedestrian i and boundary b. Equation (5) defines the force between pedestrians and boundaries.

$$\mathbf{f}_{ib}(t) = \left(A_i \exp\left[\frac{r_i - d_{ib}}{R_i} \right] + p\Theta(r_i - d_{ib}) \right) \mathbf{n}_{ib} - \kappa\Theta(r_i - d_{ib})(\mathbf{v}_i^T \cdot \mathbf{t}_{ib})\mathbf{t}_{ib} \tag{5}$$

Repulsive forces for boundaries are similar to that of dangerous obstacles but with a much stronger magnitude. The effects of this interaction are qualitative and depend on the type of boundary (fire, explosion, gas, etc.) that the pedestrian is encountering. These dangerous boundaries can limit the mobility of pedestrians depending on their exposure to it. In summary, we can describe the overall force on pedestrian i during an evacuation/panicking scenario to be as follows. For this behavior, we set $\gamma_i = 0$ in the formula for $\mathbf{f}_{ij}^{rf}(t)$. Equation (6) shows the overall forces on pedestrian i where the mass of pedestrian i is given by m_i.

$$\mathbf{f}_i(t) = m_i \frac{v_i(0)\mathbf{e}_i(0) - \mathbf{v}_i(t)}{\tau_i} + \sum_{j(\neq i)} \mathbf{f}_{ij}^{\text{rf}}(t) + \sum_{b \in B} \mathbf{f}_{ib}(t) + \sum_{j(\neq i)} \mathbf{f}_{ij}^{\text{ph}}(t) \tag{6}$$

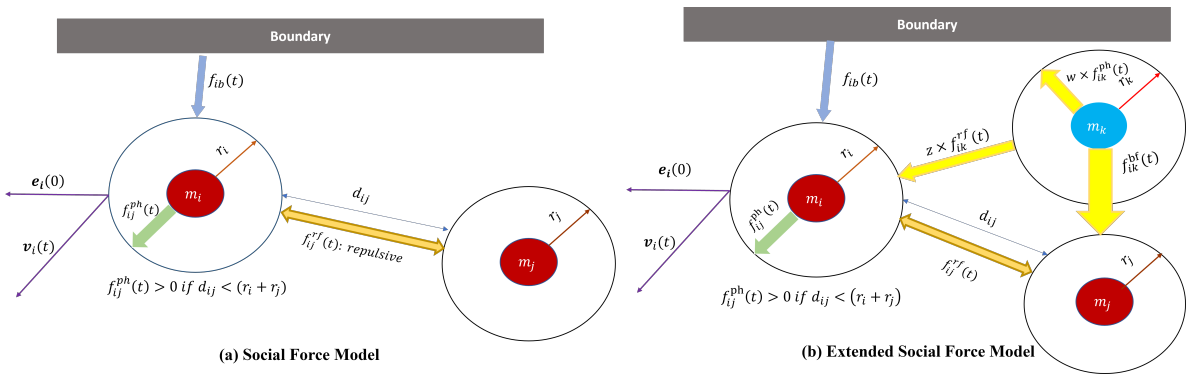

Figure 2: Illustration of SFM and E-SFM.

3.2 Extended Social Force Model: E-SFM

For the extension, the authors introduce a new variable and a coefficient to represent the law enforcement personnel as shown in Figure 2. The variable i defines the pedestrian of focus and j represents the other surrounding pedestrians of the model. To represent police officers in the formulation, we will use the index k to denote law enforcement personnel, as some forces will only be produced/modified by law enforcement. A larger modification made to the SFM that can aid in correctly modeling the crowd influence of law enforcement personnel is the bubble force $\mathbf{f}_{ik}^{\text{bf}} \in \mathbb{R}^2$. This force is meant to act as a bubble around police officers in the simulation, causing pedestrians to clear the way for them. This function will be strong as the distance between pedestrians is small, but will quickly decline as that distance grows. Since the function value starts high and declines at a faster-than-linear rate, we have chosen to use an exponential decay function (Istratov and Vyvenko 1999; Steyerl and Malik 1992) to define the bubble force $\mathbf{f}_{ik}^{\text{bf}}$ based on the distance between two people. Linear decay was also tested, but the force either reached out too far or was too weak when d_{ik} was small. Exponential decay was the best choice to model the bubble force as it can represent the quickly-decaying bubble force around the police officer.

The minimum value for this force will be 0 if d_{ik} is great enough, meaning that the law enforcement personnel k and pedestrian i are too far separated to allow the bubble force to effect the pedestrian. The maximum value for this function will be the value of the velocity vector, and will cause pedestrian i to move away from police officer k. More specifically, a pedestrian very close to the police officer will be pushed directly away from the officer's direction of motion. The sine function in Equation (7) is used to correctly model the direction of the force dependent on the relative location between the two agents. φ_{ik} represents the angle between the direction of motion of pedestrian i and officer k. The characteristic function $\chi(\sin\varphi_{ik}(t))$ then returns 1 if $(0^\circ < \varphi_{ik}(t) < 180^\circ)$, otherwise, -1, causing the direction of the resultant force vector to be flipped. This force is only produced by police officers and can be defined as shown below in Equation (7).

$$\mathbf{f}_{ik}^{\text{bf}}(t) = \chi(\sin\varphi_{ik}(t))\mathbf{v}_k(t)\exp[-d_{ik} - r_{ik}] \tag{7}$$

Equation (6) is modified to create the E-SFM. The extension includes the magnification to the repulsive force and the introduction of the bubble force. Since police officers will provide a higher magnitude repulsive force between themselves and other pedestrians $\mathbf{f}_{ij}^{\text{rf}}$, the coefficients $z > 0$ will be applied to this part. Additionally, the physical interaction force $\mathbf{f}_{ij}^{\text{ph}}$ will be stronger as they will try to direct those around them away from danger, so the coefficient $w > 0$ will be applied to this too. The interactions between pedestrian i and a boundary $\mathbf{f}_{ib}$ will remain the same, so no coefficient shall be applied to this part. The summation of the bubble force is added to the total force equation. The resultant equation is given in Equation (8).

$$\mathbf{f}_i(t) = \frac{v_i(0)\mathbf{e}_i(0) - \mathbf{v}_i(t)}{\tau_i} + \sum_{j(\neq i)} \mathbf{f}_{ij}^{\text{rf}}(t) + \sum_{b\in B} \mathbf{f}_{ib}(t) + \sum_{j(\neq i)} \mathbf{f}_{ij}^{\text{pf}}(t) + h\sum_{k\in K} \mathbf{f}_{ik}^{\text{bf}}(t) + z\sum_{k\in K} \mathbf{f}_{ik}^{\text{rf}}(t) + w\sum_{k\in K} \mathbf{f}_{ik}^{\text{pf}}(t) \tag{8}$$

To ensure that the coefficients do not change the original SFM beyond recognition, we will introduce constraints for the extended part of the model. The coefficient h for $\mathbf{f}_{ik}^{bf}(t)$ will follow a simple rule. There will only be two values for this coefficient, used to distinguish between two different types of police officers, which we explain in detail in a later section. The available values are $h = 1, 2 \;\forall\; k$ and $h = 0 \;\forall\; i, j$. As for a constraint for z, there becomes a point at which the coefficient becomes so large that it is infeasible. This constraint will be derived from experimental results and will be discussed in a later section. A constraint for the physical force coefficient w will be discussed in a later section.

Equation (8) has many components due to each pedestrian needing to sum the conventional SFM forces amongst other pedestrians, in addition to the sum of modified forces produced only by law enforcement personnel k. To obtain a simplified version of this equation as given in the previous section and from

(Pelechano and Malkawi 2008), we can write the previous equation as Equation (9).

$$\mathbf{f}_i(t) = m_i \frac{d\mathbf{v}_i}{dt} = m_i \frac{v_i(0)\mathbf{e}_i(0) - \mathbf{v}_i(t)}{\tau_i} + \sum_{j(\neq i)} \mathbf{f}_{ij} + \sum_{b \in B} \mathbf{f}_{ib} + \sum_{k \in K} (z_k \mathbf{f}_{ik}^{\mathrm{rf}} + h_k \mathbf{f}_{ik}^{\mathrm{bf}} + w_k \mathbf{f}_{ik}^{\mathrm{pf}}) \tag{9}$$

The forces between the police officers k and other pedestrians (i, j) have been magnified by the previously mentioned coefficients to increase their crowd presence. The bubble force has also been added to realistically represent a police officer's increased influence in a crowd, especially during chaotic times. The forces between any pedestrians (i, j, k) and boundaries b remain unchanged. Interactions between normal pedestrians (i, j) remain unchanged as well.

4 IMPLEMENTATION AND VALIDATION

We simulate an evacuation scenario in Mississippi State University (MSU) campus environment during a career fair event. These types of events typically attract large crowds, gathering around tables and tents. In this scenario, we assume an attack occurs (represented by an explosion), and law enforcement officers are responsible for rerouting the crowd to avoid a second potential attack area. Both the original SFM and the extended SFM are applied to model the evacuation behavior. The extended SFM specifically accounts for the increased influence of nearby police officers on the crowd. To ensure consistency with the principles of the SFM, we utilized the 3D game engine Unreal Engine, which is integrated with the NVIDIA PhysX physics engine (Dickinson et al. 2019) for the simulation as illustrated in Figure 3.

4.1 Simulation Environment

Unreal Engine was selected as the modeling platform due to its versatility in creating customized environments and its support for numerous open-source plugins. For example, the authors utilized "Cesium Ion," which integrates 3D geospatial GIS data, including terrain imagery, atmospheric and sky visuals, and 3D OpenStreetMap (OSM) buildings. This data serves as the foundation for constructing location-specific simulation environments. As shown in Figure 4, the simulation environment was developed using Unreal Engine 4.27, with a closer view of the scenes depicted. In the simulation, the white characters represent pedestrians, while the black characters represent law enforcement personnel (i.e., police officers).

In our simulation models, the agents will initially act according to the basic SFM. As a "control group," this approach will allow us to establish a baseline. For validation, we will explore different parameter levels for three forces—repulsive, bubble, and physical—to assess the police officers' influence on evacuations. The evacuation scenario involves a large group of students gathered in the central area of the campus for a career fair. During the event, an explosion occurs, causing the students to flee in search of safety. Law

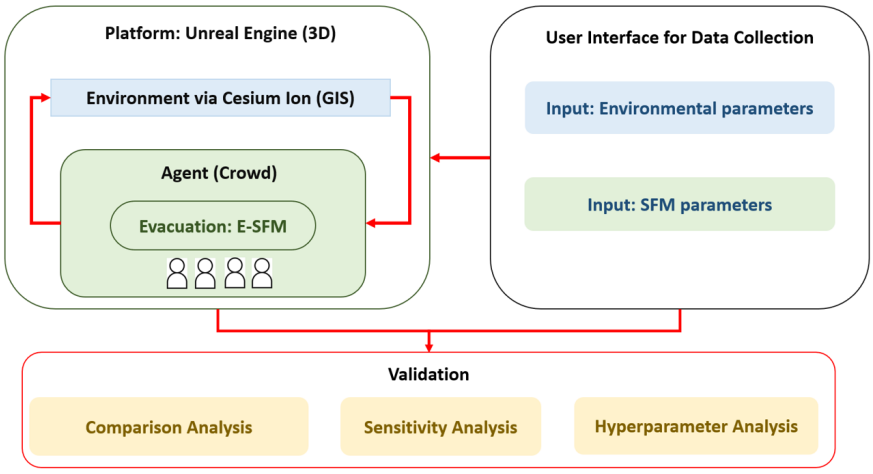

Figure 3: Overview of the simulation model implemented.

Figure 4: Simulation environments in Unreal Engine.

enforcement officers aim to prevent students from evacuating through the center of the career fair, which we assume is the most likely location for a second attack due to the high density of tables where employers and students are concentrated. Four police officers are strategically positioned around the scene to manage security. This setup allows us to test whether the extended SFM, which incorporates the influence of police officers, significantly affects the evacuation behavior of nearby students. The model's effectiveness will be assessed by counting how many pedestrians the officers successfully prevented from moving through the center of the career fair after the explosion. Tracking how many individuals pass through the designated center of the career fair will yield numerical results. This response will test the police officers' proposed heightened social forces, enabling them to move more efficiently through the crowd and steer people away from potential danger based on their strategy.

4.2 Experiment Setup for Validation

The officer k will have the forces $\mathbf{f}_{ik}^{\text{rf}}$, $\mathbf{f}_{ik}^{\text{bf}}$, and $\mathbf{f}_{ik}^{\text{pf}}$ applied to them, with the coefficients z, H and w to modify them, respectively. The goal of the police officers is to block an area of danger during an evacuation procedure. The officers will need to navigate through an evacuating crowd to reach their goal location to create the blockade. We will use the metric of the number of pedestrians allowed through this area per evacuation to determine the validity of the model.

To improve the validity of the simulation, we will incorporate two types of police officers (authoritative and passive) and three types of pedestrians (compliant, indifferent, and disobedient), similar to the modified SFM simulation in (Zhou et al. 2021). The two types of police officers reflect common police behavior in the U.S. The authoritative officer will be loud, have a stronger presence in the crowd, and exert more influence. In contrast, the passive officer will be quieter, have a socially weaker presence, and exert less influence. Regarding pedestrians, the compliant pedestrians will actively avoid police officers when spotted, prioritizing police forces over other pedestrians' forces. The indifferent pedestrians will behave like average pedestrians, treating both police officers and pedestrians similarly, but still considering the stronger influence of authoritative officers. Lastly, the disobedient pedestrians, representing individuals who do not trust police officers, will disregard police forces.

The environmental settings are incorporated into the simulation as follows: authoritative officers will generate a larger bubble force, while passive officers will have a smaller bubble force. Compliant pedestrians will place high importance on the police officers, with high coefficients for their $\mathbf{f}_{ik}$ values. Indifferent pedestrians will have lower coefficients but will still consider the bubble force when responding. Disobedient pedestrians will not respond to any $\mathbf{f}_{ik}$ values and will treat police officers as they would any other pedestrian, using $\mathbf{f}_{ij}$ values. Compliant and disobedient pedestrians each make up 10% of the crowd, while the remaining 80% are indifferent pedestrians. The distribution between passive and authoritative police officers is evenly split. After applying the E-SFM to the simulation environment, we analyzed the crowd behavior, specifically focusing on the number of pedestrians that are allowed to pass through the area of danger.

Parameter Selection The parameters z, h, and w were introduced in this study to extend the SFM. Their conceptual formulation follows the same principles of interpersonal repulsion and the influence described in (Helbing et al. 2000; Helbing et al. 2002). The parameter ranges were informed by efforts using real video-stream data as examined in (Johansson et al. 2007). In specific, we first selected initial values by analogy to the magnitudes and decay distances reported for standard repulsion forces between pedestrians, then they were further refined through exploratory calibration to ensure that simulated behaviors in Unreal Engine. For example, initially, a z value of 1 was used to reflect the original SFM behavior. We then tested z values of 15, 35, 50, 75, and 100. For each z value, 25 data points were collected. Let $\bar{X}(z)$ represent the number of pedestrians allowed into the danger area, where z corresponds to the modification applied to the SFM. The average number of pedestrians for each z value is denoted as $\bar{X}(z)$. To test the validity of the bubble force $\mathbf{f}_{ik}^{\text{bf}}(t)$, two types of officers are present in the simulation scene: passive and authoritative. The coefficient h in Equation 8 denotes the strength of the bubble force and depends on the type of police officer. A passive officer is assigned an h value of 1, while an authoritative officer is assigned an h value of 2, doubling their bubble force to reflect their increased presence and authority. Similar to the testing guidelines for the repulsive force, we will test each configuration 25 times, with a total of 4 police officers.

The random variable X_H represents the number of civilians allowed through the danger area by the police officers after the initial explosion, where H corresponds to the sum of h values in that simulation run ($H = \sum_k h_k$). For example, if there are 2 passive officers and 2 authoritative officers, then $H = 6$. If all 4 officers are passive, then $H = 4$. The maximum H value is 8, and the minimum is 1 per police officer present. The average response across 25 runs for a given H value is represented by $\bar{X}_H$. We tested the values $H = 0, 4, 5, 6, 7, 8$. Lastly, the physical force modification must be tested. To do this, we include 6 different values for w, the coefficient that modifies the physical force of police officers. We tested the values $w = 1, 5, 10, 15, 20, 25$. Unlike the bubble force, the same modification magnitude will apply to all officers on the scene. The variable X_w will represent the number of pedestrians allowed through the danger area after the initial explosion, respectively to the value of w. We then run the simulation 25 times for each value of w. The response variable measures the number of pedestrians allowed through the danger area after the initial attack. The average response value across 25 simulation runs can be represented by $\bar{X}_w$.

4.3 Extended Social Force Model Results

We first discuss the generalization of repulsive force. The repulsive force generation is illustrated in Figure 5 (left). Figure 5 shows us the average number of pedestrians allowed through the danger area per simulation run across different values of z, where H and w are held constant with values of 0 and 1, respectively. The leftmost bar represents the original SFM taken from (Helbing et al. 2002), and the 5 rightmost bars represent the E-SFM, only with different z values. The error bars on each bar represent a confidence interval constructed with 95% confidence and a sample size of $n = 25$. We can observe that the average value of the E-SFM responses fall outside the original SFM's confidence interval, indicating that the E-SFM to the repulsive force drives significant change in the evacuation patterns: The average number of pedestrians

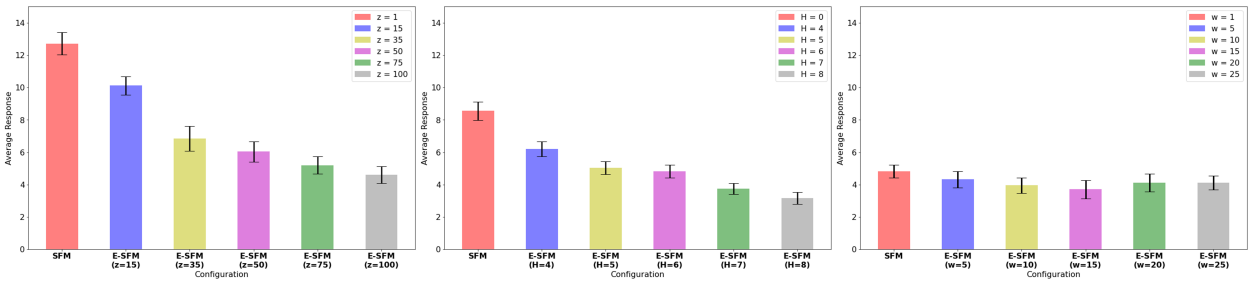

Figure 5: Repulsive force modification confidence intervals (left); Bubble force extension confidence intervals (middle); Physical force modification confidence (right).

allowed through the danger zone decreases as z increases. In specific, the bar chart displays $\bar{X}_1 = 12.72$, $\bar{X}_{15} = 10.12$, $\bar{X}_{35} = 6.84$, $\bar{X}_{50} = 6.04$, $\bar{X}_{75} = 5.2$ and $\bar{X}_{100} = 4.6$. Stronger repulsive forces between officers and pedestrians result in fewer collisions, allowing officers to reach the danger zone more quickly and block more pedestrians from passing through the potentially dangerous area.

Next, we examine the results of the generation of the bubble force $\mathbf{f}_{ik}^{\text{bf}}(t)$. As defined earlier, the variable H represents the sum of the coefficient h from equation 8. Given that there are 4 officers in the scenario, we tested values of H ranging from 4 to 8 ($H = 4,5,6,7,8$). Each H value includes 25 data points, resulting in a total of 150 data points for the bubble force extension. The variables z and w were held constant at 35 and 1, respectively. It is noted that how the introduction of the bubble force affects the evacuees' response in the middle of Figure 5. Each bar also represents the average number of pedestrians evacuated through the danger zone, with a sample size of 25. The first bar represents a value of $H = 0$, or no bubble force present (original SFM). The figure shows that as the bubble force increases, the number of evacuees passing through the danger zone decreases more rapidly. Indeed, as more bubble force is applied (representing increased law enforcement control), the number of evacuees entering the danger zone decreases, highlighting the significance of the officers' control during evacuation. The bubble force acts as a stronger influence, quickly pushing pedestrians out of the officer's path. Unlike the repulsive force, which affects both the pedestrians and the law enforcement officers, the bubble force only impacts the pedestrians, leading to a faster reduction in the $\bar{X}$ value. Pedestrians, at the same time, respond more strongly to the bubble force than the repulsive force, making larger adjustments to their paths to avoid the officers. As a result, the officers can move through the crowd more quickly, block the danger zone earlier, and prevent more pedestrians from passing.

Lastly, we discuss the extension of the physical force. Similar to the repulsive force modification, this extension involves a coefficient that increases the magnitude of the force when police officers come into contact with pedestrians. To test this modifier, we used five different values of w, the coefficient for modifying $\mathbf{f}_{\text{ik}}^{\text{ph}}(w)$: $w = 5,10,15,20,25$. The right figure in Figure 5 presents a bar chart constructed from the modification of the physical force coefficient w. The sample size for this control chart is $n = 25$, as no sample means exceeding another sample's confidence interval, meaning no significant change in response came about from modification of the physical force $\mathbf{f}_{ik}^{ph}(t)$. Indeed, as the physical forces increase, the evacuation pattern does change significantly. The reason that the physical force drives no change is that the physical force only produces values when two agents collide. As the stronger repulsive force and the newly introduced bubble force prevent collisions between officers and pedestrians, the physical force remains inactive in the presence of these forces. Therefore, this figure demonstrates that our E-SFM adheres to the basic principles of the original model while capturing law enforcement's control over the crowd.

Figure 6 illustrates the effects of the interaction between variables. These contour plots help identify which configurations of z, H, and w result in the minimum or maximum response. Red indicates a higher

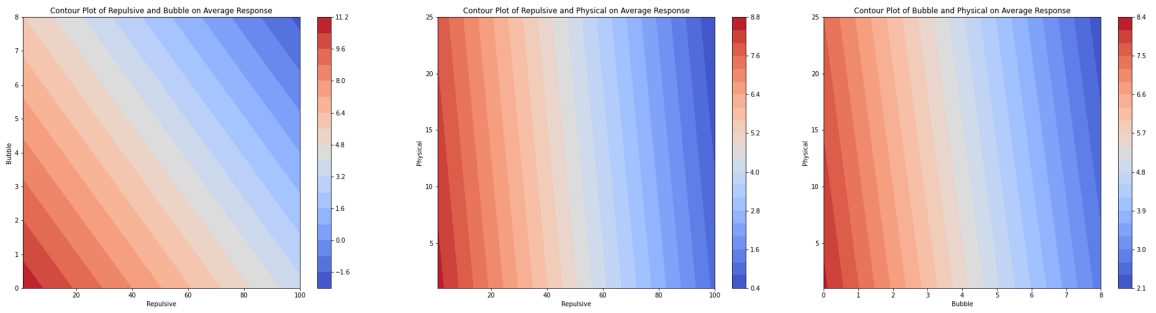

Figure 6: Contour plots - Repulsive and bubble forces vs response (left); Repulsive and phyiscal forces vs response (middle); Bubble and phyiscal forces vs response (right)

response value, while blue indicates a lower response (people evacuating through the danger zone). For our evacuation scenario, we aim to minimize the response, showing that large repulsive and bubble forces are required 6 (left). In Figures 6 (middle) and 6 (right), it is evident that the physical force $f_{ik}^{ph}(t)$ has no influence on the response variable, while the repulsive force and bubble force are the only two factors that combine to affect the response.

5 CONCLUSION AND FUTURE WORK

In conclusion, we studied the impact our E-SFM has on evacuation scenarios in a realistic event on the college campus, by incorporating the repulsive force, the physical force, and the bubble force. We validated the framework using physics-based simulation in Unreal Engine, incorporating the equations of the E-SFM to define the behavior of both pedestrians and police officers. The response variable used to evaluate the effectiveness of the SFM extensions was the number of pedestrians allowed through the "danger zone" after the initial explosion. Our results showed that the generalizations of the repulsive and bubble forces significantly influenced the evacuation behavior of law enforcement and pedestrians, while maintaining the principles of the original SFM.

Future work could extend the model by incorporating high-density interactions in high-risk environments to better capture extreme behaviors typical of stadium settings or man-made disasters. Moreover, different types of first responders, such as firefighters, paramedics, or medical personnel, can be considered to shape crowd dynamics realistically. It will be used to establish triage zones, directing movement, or eliciting varying levels of trust and compliance. Incorporating these diverse responder roles with role-specific behavioral rules would improve the model's practicality for emergency planning and training application. Another direction the authors are currently pursuing is the application of control using unmanned vehicles (UVs) and real-time detection data. By applying detection and tracking algorithms collected through UVs, the proposed SFM parameters can be updated using Bayesian approaches, enabling data-driven control strategies. The UV simulator developed in this work supports the integration of machine learning and AI algorithms into UV operations for research purposes. Accordingly, we aim to leverage the proposed simulated environment and evaluate machine learning and AI algorithms for UVs and crowd controls.

ACKNOWLEDGMENTS

This research was supported by the Bagley College of Engineering (BCoE) at Mississippi State University.

REFERENCES

Arteaga, C., J. Park, B. T. Morris, and S. Sharma. 2023. "Effect of trained evacuation leaders on victims' safety during an active shooter incident". *Safety science* 158:105967.

Cornes, F. E., G. A. Frank, and C. O. Dorso. 2021. "Microscopic dynamics of the evacuation phenomena in the context of the Social Force Model". *Physica A: Statistical Mechanics and its Applications* 568:125744.

De Cauwer, H., D. G. Barten, D. Tin, L. J. Mortelmans, G. R. Ciottone, and F. Somville. 2023. "Terrorist attacks against concerts and festivals: a review of 146 incidents in the Global Terrorism Database". *Prehospital and disaster medicine* 38(1):33–40.

Dickinson, P., K. Gerling, K. Hicks, J. Murray, J. Shearer, and J. Greenwood. 2019. "Virtual reality crowd simulation: effects of agent density on user experience and behaviour". *Virtual Reality* 23(1):19–32.

Golas, A., R. Narain, and M. C. Lin. 2014. "Continuum modeling of crowd turbulence". *Physical review E* 90(4):042816.

Han, Y., and H. Liu. 2017. "Modified social force model based on information transmission toward crowd evacuation simulation". *Physica A: Statistical Mechanics and its Applications* 469:499–509.

He, L., J. Pan, S. Narang, W. Wang, and D. Manocha. 2016. "Dynamic group behaviors for interactive crowd simulation". *arXiv preprint arXiv:1602.03623*.

Helbing, D., I. Farkas, and T. Vicsek. 2000. "Simulating dynamical features of escape panic". *Nature* 407(6803):487–490.

Helbing, D., I. J. Farkas, P. Molnar, and T. Vicsek. 2002. "Simulation of pedestrian crowds in normal and evacuation situations". *Pedestrian and evacuation dynamics* 21(2):21–58.

Helbing, D., and P. Molnar. 1995. "Social force model for pedestrian dynamics". *Physical review E* 51(5):4282.

Huang, L., J. Gong, W. Li, T. Xu, S. Shen, J. Liang, *et al*. 2018. "Social force model-based group behavior simulation in virtual geographic environments". *ISPRS International Journal of Geo-Information* 7(2):79.

Istratov, A. A., and O. F. Vyvenko. 1999. "Exponential analysis in physical phenomena". *Review of Scientific Instruments* 70(2):1233–1257.

Johansson, A., D. Helbing, and P. K. Shukla. 2007. "Specification of the social force pedestrian model by evolutionary adjustment to video tracking data". *Advances in complex systems* 10(supp02):271–288.

Kolivand, H., M. S. Rahim, M. S. Sunar, A. Z. A. Fata, and C. Wren. 2021. "An integration of enhanced social force and crowd control models for high-density crowd simulation". *Neural Computing and Applications* 33:6095–6117.

Liu, P., Q. Chao, H. Huang, Q. Wang, Z. Zhao, Q. Peng, *et al*. 2022. "Velocity-based dynamic crowd simulation by data-driven optimization". *The Visual Computer* 38(9):3499–3512.

Lu, P., Y. Li, F. Wen, and D. Chen. 2023. "Agent-based modeling of mass shooting case with the counterforce of policemen". *Complex & Intelligent Systems* 9(5):5093–5113.

Luo, L., S. Zhou, W. Cai, M. Y. H. Low, F. Tian, Y. Wang, *et al*. 2008. "Agent-based human behavior modeling for crowd simulation". *Computer Animation and Virtual Worlds* 19(3-4):271–281.

Narain, R., A. Golas, S. Curtis, and M. C. Lin. 2009. "Aggregate dynamics for dense crowd simulation". In *ACM SIGGRAPH Asia 2009 papers*, 1–8.

Ondřej, J., J. Pettré, A.-H. Olivier, and S. Donikian. 2010. "A synthetic-vision based steering approach for crowd simulation". *ACM Transactions on Graphics (TOG)* 29(4):1–9.

Pelechano, N., and A. Malkawi. 2008. "Evacuation simulation models: Challenges in modeling high rise building evacuation with cellular automata approaches". *Automation in construction* 17(4):377–385.

Pettré, J., D. Wolinski, and A.-H. Olivier. 2014. "Velocity-based models for crowd simulation". In *Pedestrian and Evacuation Dynamics 2012*, 1065–1078. Springer.

Prasithsangaree, P., J. M. Manojlovich, J. Chen, and M. Lewis. 2003. "UTSAF: a simulation bridge between OneSAF and the Unreal game engine". In *SMC'03 Conference Proceedings. 2003 IEEE International Conference on Systems, Man and Cybernetics. Conference Theme-System Security and Assurance (Cat. No. 03CH37483)*, Volume 2, 1333–1338. IEEE.

Steyerl, A., and S. Malik. 1992. "Possible implications of exponential decay". *Annals of Physics* 217(2):222–278.

Stokols, D. 1972. "A social-psychological model of human crowding phenomena". *Journal of the American Institute of Planners* 38(2):72–83.

Wan, J., J. Sui, and H. Yu. 2014. "Research on evacuation in the subway station in China based on the Combined Social Force Model". *Physica A: Statistical Mechanics and its Applications* 394:33–46.

Wei-Guo, S., Y. Yan-Fei, W. Bing-Hong, and F. Wei-Cheng. 2006. "Evacuation behaviors at exit in CA model with force essentials: A comparison with social force model". *Physica A: Statistical Mechanics and its Applications* 371(2):658–666.

Xin, Y.-L., G.-P. Ge, W. Du, H. Wu, and Y. Zhao. 2024. "Design of an Optical Physics Virtual Simulation System Based on Unreal Engine 5". *Applied Sciences* 14(3):955.

Xing, W., J. Zhang, W. Lu, and P. Bao. 2015. "An Improved Potential Field Based Method for Crowd Simulation". *International Journal of Software Engineering and Knowledge Engineering* 25(03):427–451.

Xiong, M., M. Lees, W. Cai, S. Zhou, and M. Y. H. Low. 2009. "A rule-based motion planning for crowd simulation". In *2009 International Conference on CyberWorlds*, 88–95. IEEE.

Yang, S., T. Li, X. Gong, B. Peng, and J. Hu. 2020. "A review on crowd simulation and modeling". *Graphical Models* 111:101081.

Zhang, P., H. Liu, and Y.-h. Ding. 2015. "Crowd simulation based on constrained and controlled group formation". *The Visual Computer* 31:5–18.

Zhang, X., Y. Fan, H. Liu, Y. Zhang, and Q. Sha. 2023. "Design and implementation of autonomous underwater vehicle simulation system based on moos and unreal engine". *Electronics* 12(14):3107.

Zhou, R., Y. Cui, Y. Wang, and J. Jiang. 2021. "A modified social force model with different categories of pedestrians for subway station evacuation". *Tunnelling and Underground Space Technology* 110:103837.

AUTHOR BIOGRAPHIES

AARON LEGRAND is a process and logistics engineer at J.B. Hunt Transport Services, Inc. He obtained his BS and MS degree in the Department of Industrial Engineering at Mississippi State University. His research interests include reinforcement learning, physics-based simulations of crowd evacuations, and Unmanned Aerial Vehicle (UAV) surveillance simulations. His email address is awl139@msstate.edu.

SEUNGHAN LEE is an assistant professor in the Industrial and Systems Engineering Department at Mississippi State University. His research encompasses modeling and analysis of data-driven systems under uncertainty using simulation and stochastic methods. Major application areas include disaster relief and mitigation efforts, smart city and homeland security, and healthcare operations. His email address is slee@ise.msstate.edu and his website is https://sites.google.com/view/sistomsu.